Journal of Sound and Vibration (1998) **216**(1), 107–132
Article No. sv981691

NOISE RADIATION FROM ENGINE COOLING FANS

S. F. Wu, S. Su

Department of Mechanical Engineering, *Wayne State University*, *Detroit*, *MI* 48202, *U.S.A.*

AND

H. Shah

Sheldon Road Plant, *Visteon Automotive*, 14425 *Sheldon Road*, *Plymouth*, *MI* 48170, *U.S.A.*

(*Received* 9 *October* 1997, *and in final form* 13 *April* 1998)

The semi-empirical formulation previously derived by the authors (*Journal of Sound and Vibration* **200**, 379–399) for predicting noise spectra of axial flow fans running in a free field is extended to engine cooling fans installed in full-size vehicles. Because of the presence of shroud, upstream radiator/condenser, and downstream engine block, the ingested and discharged flow fields around the fan blades are completely different from those in a free field. Accordingly, the noise generation mechanisms become much more difficult to analyze and model. The shroud may significantly increase the unsteady fluctuating forces exerted on the fan blades, thus greatly enhancing the levels of the discrete sounds centered at the blade passage frequency and its harmonics. The upstream radiator/condenser set may induce a significant amount of intake turbulence, thus raising the levels of the broadband sounds. The downstream engine block may force the airflow to recirculate to the front and more importantly, raise the static pressure drop across the fan assembly, which has a direct impact on the resulting flow rate. Obviously, an exact description of the effects of these factors on the resulting noise spectra is not possible. In this paper it is shown that these factors can be approximated by using certain shape functions. The computer model thus developed is used to predict the noise spectra from different fan assemblies under various working conditions, and the results thus obtained are compared with the measured data. Also, this model is used to calculate the overall sound pressure levels from dimensionally similar fans running under different working conditions, and the results are compared with those predicted by the fan laws currently in use by engineers in the automotive industry.

1. INTRODUCTION

Engine cooling fans have long been recognized as one of the major noise sources in a vehicle. As the engine and other vehicle components are made quieter, the need to reduce fan noises has become more and more urgent. To reduce fan noises in a cost-effective manner, it is necessary to incorporate the component of noise reduction into an early design stage. For this purpose, we must develop a computer model that will allow design engineers to estimate the noise spectra and overall sound pressure level (SPL) values, given the characteristic dimensions and working conditions of a fan assembly.

In a previous paper [1], the authors developed a semi-empirical formula for predicting the noise spectrum of an axial flow fan in an unobstructed flow field. The basic assumption made in deriving this formula is that fan noises are primarily caused by fluctuating forces exerted on the surrounding fluid medium by rotating blades. This fluid/structure

0022–460X/98/360107 + 26 $30.00/0

interaction results in discrete sounds centered at the blade passage frequency (BPF) and its harmonics.

This sound generation mechanism has been known for more than 30 years [2–20]. Nonetheless, an exact solution to this fluid/structure interaction still cannot be found to date. In many applications, one still relies on empirical formulae to estimate the overall SPL values of given fan models. Such an estimation is often insufficient to characterize the noise performance, because the fan noises contain both narrow band and broadband sounds, and the latter has a masking effect and carries the majority of acoustic energy. Hence, it is desirable to be able to predict the spectrum of an engine cooling fan.

In this paper, the semi-empirical model developed previously by the authors [1] is extended to prediction of noise radiation from an engine cooling fan assembly installed in a full-size vehicle. Experimental results demonstrate that the noise characteristics of an engine cooling fan assembly are distinctly different from those of an axial flow fan in a free field. First, a shroud can generate a significant amount of unsteady fluctuating forces, thus enhancing the discrete sounds. Second, an upstream radiator/condenser set induces intake turbulence, thus increasing the broadband noise level. Third, the upstream radiator/condenser and downstream engine block raise the static pressure drop across the fan assembly, which has a direct impact on the resulting flow rate. These factors are taken into account in a computer model presented in section 3. The computer model thus developed is used to calculate noise spectra from five different engine cooling fan assemblies running under various working conditions. Section 4 displays the experimental set-up for validating this computer model. Comparisons of the calculated and measured noise spectra are displayed in section 5. As a further check of its validity, this computer model is used to calculate the overall SPL values from three sets of dimensionally similar fans subject to various speeds, flow rates, and static pressure drops changes. The results thus obtained are compared with those predicted by the fan laws currently in use by engineers in the automotive industry (see section 6). The conclusions are drawn in section 7.

2. FORMULATION FOR AN AXIAL FLOW FAN IN A FREE FIELD

The semi-empirical formula developed previously by the authors [1] for predicting noise spectra of an axial flow fan running in a free field is given by

$$sp = \sum_{n=0}^{\infty} \mathrm{Re}\,[SP_n \mathscr{H}_n(f)\, \mathrm{e}^{-i2\pi nBf_0 t}], \tag{1}$$

where SP_n represents the amplitude of the nth narrow band of the noise spectrum

$$SP_n = \int_{r_h}^{r_t} \frac{27{\cdot}4\rho C_L \mathscr{C} V_o^2 B^2 [0{\cdot}96739(1-\xi_b) - 0{\cdot}2924] \cos\psi \sin\theta \sin(\psi-\beta)}{16\pi^2 R_o [1 - 0{\cdot}0217(1-\xi_b)(f/f_o)\sin(\gamma_h - \gamma)]}$$

$$\times (1 - \mathrm{e}^{-54{\cdot}8\pi r/B}) \left(i\frac{2\pi nBf_o}{c} - \frac{1}{R_o} \right) \frac{(2-\delta_{0n})\, \mathrm{e}^{i2\pi nBf_o\sqrt{R_o^2+r^2}/c}}{(27{\cdot}4r)^2 + (nB)^2}\, r\, \mathrm{d}r, \tag{2}$$

and $\mathscr{H}_n$ in equation (1) is the shape function for the nth narrow band whose amplitude is unity at the center frequency of the band, but decays exponentially as the frequency deviates from the center frequency

$$\mathscr{H}_n(f) = \left(1 - \left|\frac{f - nf_o}{f_o}\right|\right) H[f - (n-1)f_o] H[(n+1)f_o - f]\, \mathrm{e}^{-(f - nf_o/f_o\sigma_n)^2}, \tag{3}$$

where H is the Heaviside step function

$$H(f - nf_o) = \begin{cases} 0, & \text{if } f < nf_o; \\ 1, & \text{if } f \geqslant nf_o; \end{cases} \tag{4}$$

and σ_n represents the decay rate of the nth narrow band given by

$$\sigma_n = \frac{n}{5}, \tag{5}$$

where n is the number of bands.

The shape functions given by equations (3) to (5) enable one to approximate the narrow bands centered at the BPF and its harmonics. In particular, the widths of these narrow bands increase with the frequency and merge to form a broadband-like spectrum at high frequencies.

In equation (2), C_L is the lift coefficient defined by [21]

$$C_L = 5{\cdot}73 \sin(\psi - \beta), \tag{6}$$

where β is the blade inclination angle at radius r and ψ is given by

$$\psi = \tan^{-1}\left(\frac{\kappa}{r}\right), \tag{7}$$

where

$$\kappa = \frac{\mathrm{CFM}}{2\pi^2 f(r_t^2 - r_h^2)}, \tag{8}$$

where CFM represents the required flow rate (ft^3/min); r_t and r_h are the tip and hub radii of the fan blade, respectively. The quantity V_o^2 in equation (2) is the mean-squared flow velocity

$$V_o^2 = 4\pi^2 f^2 (r^2 + \kappa^2). \tag{9}$$

The symbol ξ_b in equation (2) is the solidity of the blade surface defined as

$$\xi_b = \frac{B}{\pi(r_t^2 - r_h^2)} \int_{r_h}^{r_t} \mathscr{C} \cos\beta \, \mathrm{d}r, \tag{10}$$

where B is the number of blades and $\mathscr{C}$ is the blade chord length at radius r. The quantities θ and R_o represent the polar co-ordinates of the measurement point

$$\theta = \tan^{-1}\left(\frac{y}{x}\right), \qquad R_o = \sqrt{x^2 + y^2}, \tag{11a, b}$$

where x and y are the horizontal and vertical distances measured with respect to the center of the fan disk.

Finally, the quantity γ_h and γ in equation (2) are the blade skew angles at the hub r_h and at radius r, respectively, ρ is the density of the fluid medium, δ_{ij} is the Kronecker delta, $f_o = NB/60$ is the BPF, and N is the fan speed.

3. EXTENSION TO ENGINE COOLING FANS

For most U.S. passenger vehicles, the engine cooling fan is installed inside a shroud with a radiator/condenser set placed in the upstream (known as the "pull-in" type fan), and an engine block in the downstream. The shroud is designed to guide the ingested airflow and to provide certain protection for the mechanics in inspecting an engine compartment under an operating condition. Because of the compactness of an engine compartment, the shroud extension covers are often made asymmetric. As a result, the ingested airflow is greatly distorted and a significant amount of unsteady fluctuating forces are generated. These unsteady fluctuating forces are much more effective in generating aerodynamic sounds than the steady fluctuating forces. Experimental results demonstrate that the presence of a shroud significantly increases the levels of discrete sounds centered at the BPF and its harmonics.

When a radiator/condenser set is placed in the upstream of a fan/shroud assembly, the ingested airflow becomes not only asymmetric, but also turbulent after passing through many tiny irregularly-shaped slots built in the radiator and condenser. Experimental results show that an intake turbulence tends to reduce the coherence of the unsteady fluctuating forces generated by a shroud, thus reducing its effectiveness in generating the discrete sounds. On the other hand, it increases the levels of the broadband sounds. Consequently, the levels of the discrete sounds are lowered slightly but their bandwidths are widened.

The flow field generated by this fan-shroud-radiator/condenser assembly is further complicated by an engine block situated in the downstream. The compactness of an engine compartment forces the discharged airflow to recirculate to the intake of the fan assembly, making it possible to generate the so-called "chopping" sounds. More importantly, this compactness raises the static pressure drop across the fan assembly, which has a direct impact on the resulting flow rate. Experimental results show that for a fixed power input, an increase in the static pressure drop reduces the fan speed and the overall flow rate, thus impairing its cooling performance. However, measurement data also indicate that the increase in the static pressure drop across a fan assembly has little impact on the overall noise spectra.

Obviously, it is unrealistic to attempt to model the entire flow field surrounding an engine cooling fan assembly as described above. Hence, analytic solutions cannot be obtained even with the use of the most sophisticated computers to date. Yet, estimations of the noise spectra from an engine cooling fan assembly are desired, especially in an early design stage to reduce resulting noise radiation in a cost-effective manner.

In what follows, an engineering computer model based on equation (1) for estimating noise spectra of an engine cooling fan assembly is presented. In this computer model, the effect of the unsteady fluctuating forces on the discrete sounds generated by a shroud, that of intake turbulence on the broadband sounds caused by an upstream radiator/condenser set, and that of changes in the static pressure drop due to the compactness of an engine compartment on the resulting noise spectra are taken into account. These effects are modelled by using certain shape functions that can best approximate the changes in the resulting spectra. The amplitudes of these shape functions are determined experimentally

through curve fitting the measured data from different fan assemblies subject to various working conditions:

$$sp = \sum_{n=0}^{\infty} PD(NB_n + BB_n)\,\mathrm{Re}\,[SP_n \mathscr{H}_n(f)\,\mathrm{e}^{-i2\pi nBf_o t}], \tag{12}$$

where NB_n accounts for the effect of the unsteady fluctuating forces generated by a shroud on the narrow band sounds centered at the BPF and its harmonics.

$$NB_n = a_1[1 + a_2(f_n/f_o)]^{-1}, \tag{13}$$

and BB_n describe the effect of incident turbulence on the broadband sounds induced by an upstream radiator/condenser set

$$BB_n = a_3[1 + a_4(f_n/f_o)]^{-1}. \tag{14}$$

The function PD in equation (12) depicts the effect of the static pressure drop across the fan assembly induced by an engine compartment,

$$PD = 10^{0{\cdot}15(\Delta p + 0{\cdot}19)}, \tag{15}$$

where Δp is the static pressure drop across the fan assembly (inch-water), which is prescribed by the pressure/flow characteristic curve of a fan. The parameters a_i, $i = 1$–4, depend on the design parameters of the shroud, radiator, and condenser. In the present model they are determined by curve fitting experimental data for all fan assemblies subject to various working conditions conducted in the Acoustics, Vibration, and Noise Control (AVNC) Laboratory at Wayne State University. Table 1 lists these experimentally determined values of a_i for both straight and back-skewed fans with a shroud and with a shroud and a radiator/condenser set, respectively. Figure 1 illustrates the flow chart of the computer model thus developed.

Note that the present computer model should be viewed as an approximation to an extremely complex aeroacoustic problem. It represents a first generation computer model that enables the design engineers to assess the noise performance of an engine cooling fan assembly. Needless to say, it is not a generalized model because many coefficients are fixed as constants. To generalize this model, it will be necessary to correlate the constants such as a_i, $i = 1$–4, to the designs of shroud, radiator/condenser, and the spacing of an engine compartment.

TABLE 1

Values of a_i for straight and back-skewed blades

	Straight blade		Skewed blade	
a_i	Fan with shroud	Fan with shroud and radiator/condenser	Fan with shroud	Fan with shroud and radiator/condenser
a_1	4·600	3·10	4·35	4·35
a_2	6·600	5·10	5·80	11·00
a_3	0·450	1·00	0·34	0·50
a_4	0·093	0·93	0·16	0·40

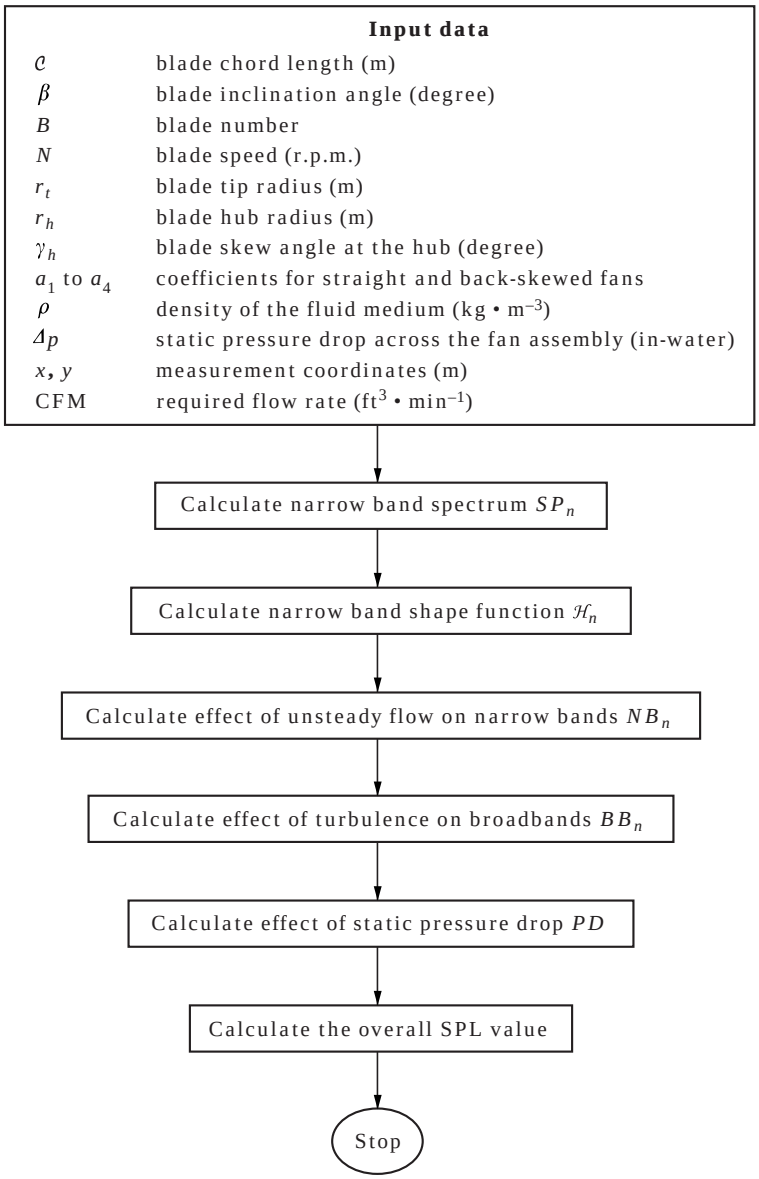

Figure 1. Flow chart for predicting noise spectra of an engine cooling fan assembly.

4. EXPERIMENTAL SET-UP

Figure 2 shows the experimental set-up for validating the computer model thus developed. The wood-framed box covered with Mylar sheets is designed and built to simulate the static pressure drop across the fan assembly due to the compactness of an engine compartment in a full-size vehicle. Since Mylar is transparent to sound waves but impermeable to airflow, it has a minimum effect on the fan noises.

In the experiments the airflow is drawn into the box through an adjustable door across the fan assembly and discharged directly to the outside. The desired static pressure drops are obtained by adjusting the opening of the doorway and monitored by a digital

barometer. The fan is driven by an HP DC power supplier and the fan speed is monitored by a laser speedometer.

The fan noise spectra are measured by a B&K Prepolarized Free-field Condenser Microphone Type 4189 at both upstream and downstream positions. The noise signals are analyzed by a B&K Dual Channel Analyzer Type 2032 and recorded in an IBM PC. The data acquisition and processing are controlled by an IBM PC computer using the StarAcoustics software. The experiments are conducted in a walk-in size ($12' \times 12' \times 6{\cdot}5'$), fully anechoic chamber in the AVNC Laboratory at Wayne State University. Some noise spectral data are measured independently by the engineers at the Robert Bosch Company in Boston for comparisons.

5. VALIDATION RESULTS

In this section, comparisons of the calculated and measured noise spectra from five completely different fan assemblies are demonstrated. For proprietary reasons, the details of the designs of the fans, shrouds, and radiator/condenser sets are omitted and the fans are simply termed as Types A, B, C, D, and E.

In what follows, first the comparisons of the calculated and measured noise spectra for Types A and B fans mounted on the wood-framed box are demonstrated, as shown in Figure 2. For each fan assembly, the cases of a fan with a shroud and a fan with a shroud and radiator/condenser set are considered, respectively. Measurements of the noise spectra from Types A and B fans are conducted in the AVNC Laboratory at Wayne State University.

Next, the calculated noise spectra from Types C, D and E fans are compared with those measured independently by the Bosch engineers. Note that the Bosch engineers measured noise spectra for these fans with shrouds only. Accordingly, the spectra for these fan assemblies, subject to the same working conditions as those specified by the Bosch engineers, are calculated.

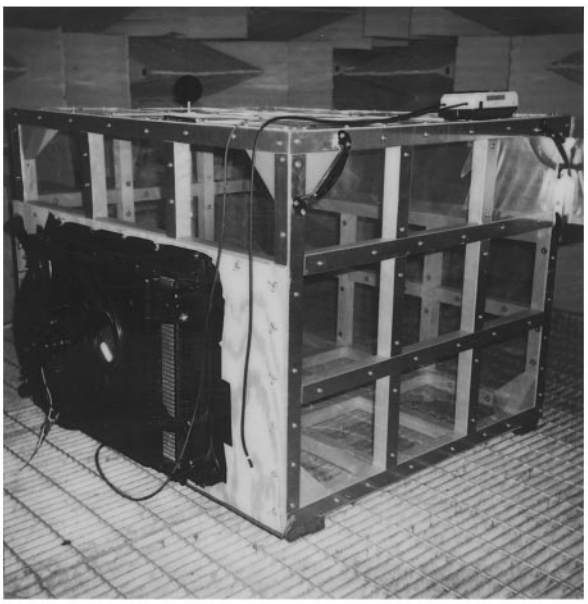

Figure 2. Experimental set-up of a cooling fan assembly mounted on a wood-framed box covered with Mylar sheet.

Figure 3. Experimental set-up for Type A fan with a shroud.

Since the cooling fans are designed to run at two speed regimes (high and low), the noise spectra are measured with fans running in both speed regimes. For brevity, however, only one comparison in each speed regime for each fan assembly are displayed in this paper. The differences in the SPL values for the discrete sounds and overall sounds are summarized in Tables 2–15.

5.1. TYPE A FAN

Type A fan is a production fan used in a four-door sedan with nine back-skewed blades. Figure 3 shows the set-up for Type A fan with a shroud. Figure 4 depicts the comparison of the calculated and measured noise spectra from Type A fan with a shroud running in the high speed regime. Table 2(a) lists the measurement co-ordinates, flow rate, static

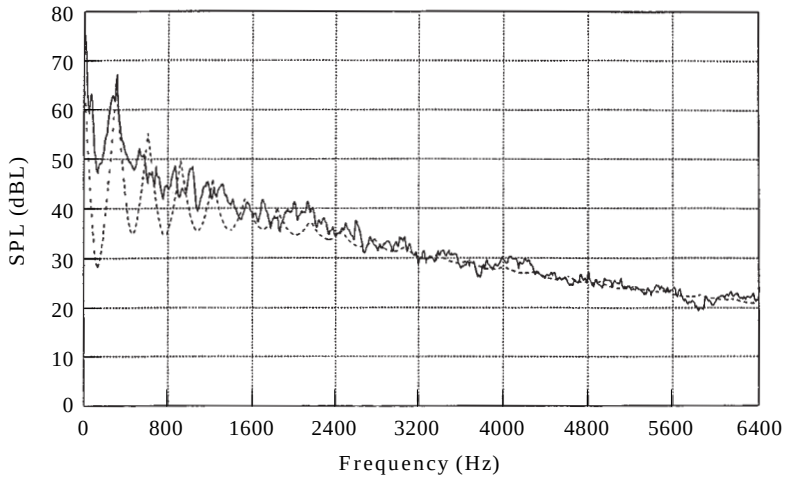

Figure 4. Comparison of the calculated and measured noise spectra from Type A fan with a shroud running in the high speed regime: —, measured; - - - , calculated.

TABLE 2(a)

Summary of the working condition for Type A fan with a shroud running in the high speed regime

Measurement location		Working conditions		
x (m)	y (m)	Flow rate (CFM)	Δp (inch-water)	Speed (r.p.m.)
2·0	0·5	2034	0·495	2052

TABLE 2(b)

Summary of the calculated and measured first two discrete sounds and the overall SPL values for Type A fan with a shroud running in the high speed regime

Peak number	Frequency (Hz)	Measured SPL (dBL)	Calculated SPL (dBL)	Difference SPL (dBL)
1	307·8	67·3	65·4	−1·9
2	615·6	50·5	55·9	+5·4
Total SPL (dBA)	0 ~ 6400	68·7	68·3	−0·4

pressure drop, and fan speed. Table 2(b) summarizes the SPL values of the first two discrete sounds and those of the overall sounds. Results show that the present computer model captures the characteristics of Type A fan noise spectra. In particular, the difference between the calculated and the measured overall SPL values is less than 0·5 dB.

Figure 5 displays the comparison of the noise spectra with Type A fan running in the low speed regime. The corresponding measurement co-ordinates, the working conditions, the differences in the first two discrete sounds and in the overall SPL values are listed in Tables 3(a) and (b), respectively.

Figures 6 and 7 plot the comparisons of the calculated noise spectra with those measured from Type A fan with a shroud and radiator/condenser assembly running in the high and

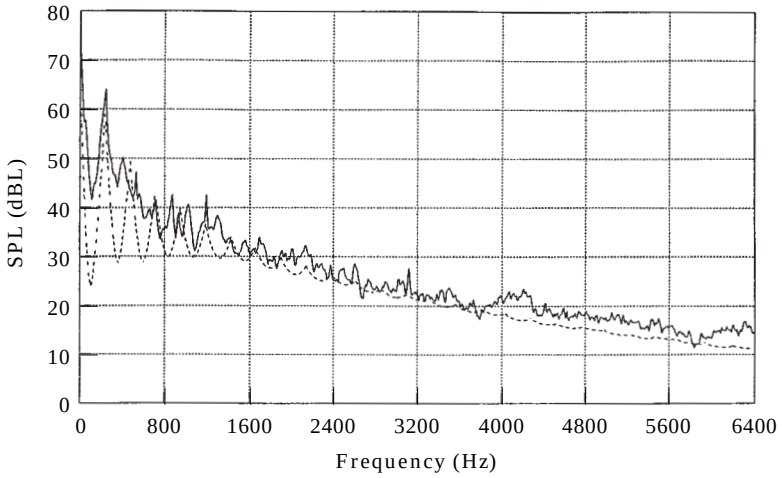

Figure 5. Comparison of the calculated and measured noise spectra from Type A fan with a shroud running in the low speed regime: —, measured; - - - , calculated.

TABLE 3(a)

Summary of the working condition for Type A fan with a shroud running in the low speed regime

Measurement location		Working conditions		
x (m)	y (m)	Flow rate (CFM)	Δp (inch-water)	Speed (r.p.m.)
2·0	0·5	1105	0·309	1584

TABLE 3(b)

Summary of the calculated and measured first two discrete sounds and the overall SPL values for Type A fan with a shroud running in the low speed regime

Peak number	Frequency (Hz)	Measured SPL (dBL)	Calculated SPL (dBL)	Difference SPL (dBL)
1	237·6	64·1	59·3	−4·8
2	475·2	50·3	49·7	−0·6
Total SPL (dBA)	0 ~ 6400	62·2	59·7	−2·5

low speed regimes, respectively. The corresponding working conditions for these cases are listed in Tables 4(a) and 5(a), respectively, and the differences in the first two discrete sounds and in the overall SPL values are summarized in Tables 4(b) and 5(b), respectively. Satisfactory results are obtained in all cases.

5.2. TYPE B FAN

Type B fan is a production fan used in a mini-van with nine straight blades. Figure 8 shows the set-up for Type B fan with a shroud. Using the company supplied blade geometries and dimensions, the spectra from Type B fan with a shroud running at both high and low speeds are calculated. The results thus obtained are compared with the measured ones (see Figures 9 and 10). Tables 6(a–b) and 7(a–b) list the corresponding flow

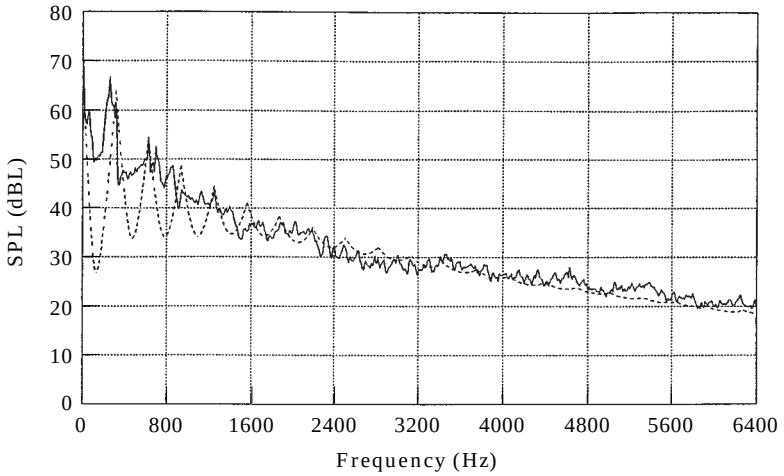

Figure 6. Comparison of the calculated and measured noise spectra from Type A fan with a shroud and radiator/condenser assembly running in the high speed regime: —, measured; - - - , calculated.

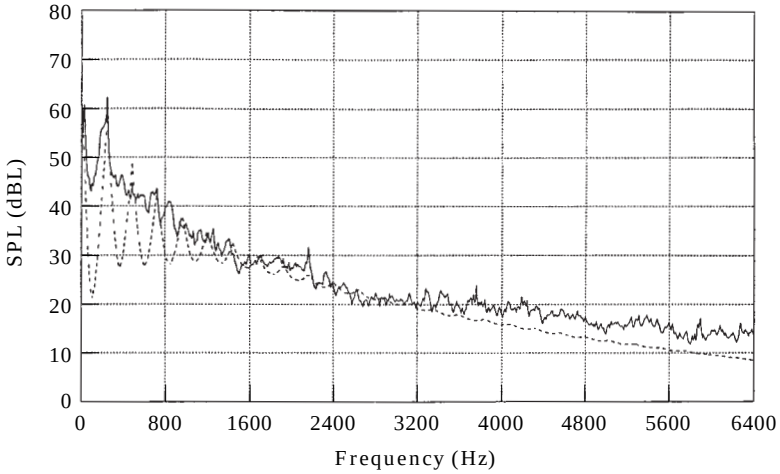

Figure 7. Comparison of the calculated and measured noise spectra from Type A fan with a shroud and radiator/condenser assembly running in the low speed regime: —, measured; - - - , calculated.

rates, static pressure drops, speeds, and differences between the calculated and measured SPL values for the first two discrete sounds and the overall sounds. As in the case of Type A fan, the computer model captures the characteristics of Type B fan noise spectra. The agreements between the calculated and measured spectra are satisfactory. In particular, the differences between the calculated and measured total SPL values are less than 1 dB.

Figures 11 and 12 illustrate the comparisons of the calculated and measured noise spectra from Type B fan with a shroud and radiator/condenser assembly running at both high and low speeds, respectively. Tables 8(a–b) and 9(a–b) illustrate the corresponding working conditions and differences between the calculated and measured SPL values for the first two discrete sounds and the overall sounds, respectively. Good agreements are obtained in all cases.

TABLE 4(a)

Summary of the working condition for Type A fan with a shroud and radiator/condenser assembly running in the high speed regime

Measurement location		Working conditions		
x (m)	y (m)	Flow rate (CFM)	Δp (inch-water)	Speed (r.p.m.)
2·0	0·5	2108	0·478	2088

TABLE 4(b)

Summary of the calculated and measured first two discrete sounds and the overall SPL values for Type A fan with a shroud and radiator/condenser assembly running in the high speed regime

Peak number	Frequency (Hz)	Measured SPL (dBL)	Calculated SPL (dBL)	Difference SPL (dBL)
1	313·2	66·8	64·4	−2·4
2	626·4	54·2	54·9	+0·7
Total SPL (dBA)	0 ~ 6400	67·4	67·4	0·0

TABLE 5(a)

Summary of the working condition for Type A fan with a shroud and radiator/condenser assembly running in the low speed regime

Measurement location		Working conditions		
x (m)	y (m)	Flow rate (CFM)	Δp (inch-water)	Speed (r.p.m.)
2·0	0·5	1650	0·114	1600

TABLE 5(b)

Summary of the calculated and measured first two discrete sounds and the overall SPL values for Type A fan with a shroud and radiator/condenser assembly running in the low speed regime

Peak number	Frequency (Hz)	Measured SPL (dBL)	Calculated SPL (dBL)	Difference SPL (dBL)
1	240·0	62·3	58·6	−3·7
2	480·0	44·0	49·1	+5·1
Total SPL (dBA)	0 ~ 6400	60·4	59·0	−1·4

5.3. TYPE C FAN

Type C fan is a production fan similar to Type A with nine back-skewed blades, but with different dimensions and geometries. To check the validity of the present computer model, Ford Motor asked the engineers at the Robert Bosch Company in Boston to conduct the noise measurements, while providing the AVNC Laboratory with the design parameters and operating conditions under which Type C fan was run. The measurements

Figure 8. Experimental set-up for Type B fan with a shroud.

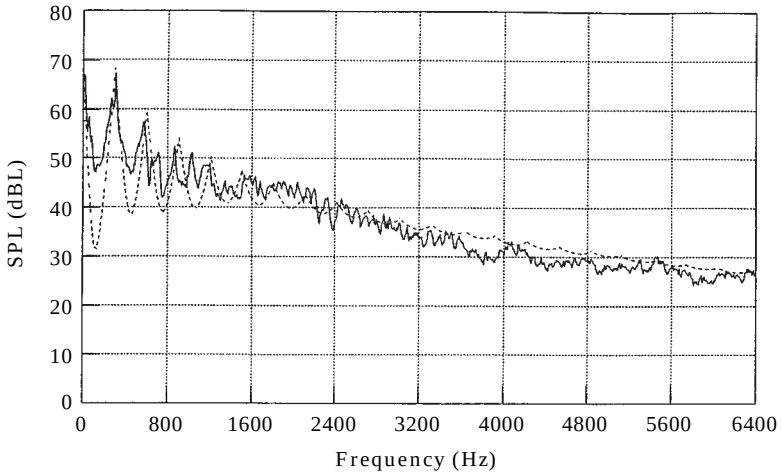

Figure 9. Comparison of the calculated and measured noise spectra from Type B fan with a shroud running in the high speed regime. —, measured; - - - , calculated.

were taken in a hemi-anechoic chamber using spatial average over a rectangular area at 1 m away from the fan module. Since the Bosch engineers only measured the noise spectra of Type C fan with a shroud, no comparisons with a shroud and a radiator/condenser set were made.

Tables 10(a–b) and 11(a–b) display the differences between the calculated and measured SPL values of the BPF and overall sounds in A-weighting for Type C fan running in both high and low speed regimes.

5.4. TYPE D FAN

Type D is a production fan similar to Type B with nine straight blades, but different geometries and dimensions. As in the case of Type C fan, Ford Motor asked Bosch engineers to conduct all the noise spectra measurements while provided the AVNC Laboratory with the pertinent blade design parameters and the working conditions under

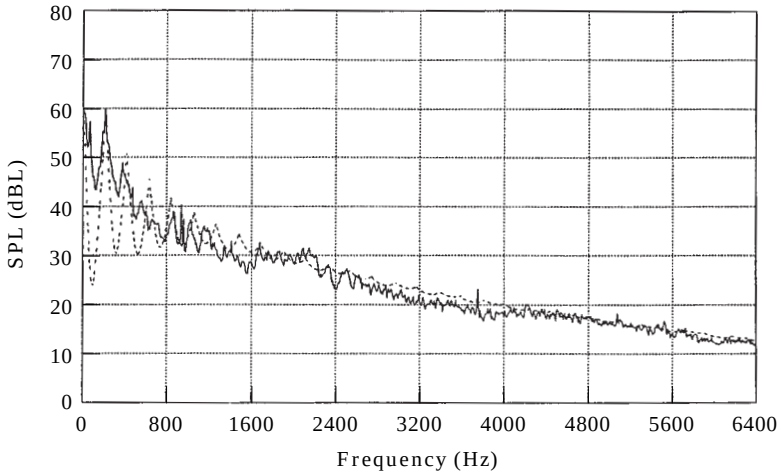

Figure 10. Comparison of the calculated and measured noise spectra from Type B fan with a shroud running in the low speed regime. —, measured; - - - , calculated.

TABLE 6(a)

Summary of the working condition for Type B fan with a shroud running in the high speed regime

Measurement location		Working conditions		
x (m)	y (m)	Flow rate (CFM)	Δp (inch-water)	Speed (r.p.m.)
2·0	0·5	1890	0·358	2039

TABLE 6(b)

Summary of the calculated and measured first two discrete sounds and the overall SPL values for Type B fan with a shroud running in the high speed regime

Peak number	Frequency (Hz)	Measured SPL (dBL)	Calculated SPL (dBL)	Difference SPL (dBL)
1	305·9	67·1	69·1	+2·0
2	611·7	58·2	60·1	+1·9
Total SPL (dBA)	0 ~ 6400	71·9	72·8	+0·9

which Type D fan was run. Tables 12(a–b) and 13(a–b) list the summaries of the measurement location and working condition, as well as the SPL values of the BPF and overall sounds in A-weighting.

5.5. TYPE E FAN

Type E fan is a prototype model that has six back-skewed blades with much larger overall dimensions than Types A, B, C and D fans, and with different inclination and back-skewed angles. Measurements of noise spectra in both high and low speed regimes were conducted by the Bosch engineers. Using the company supplied input data, the noise

TABLE 7(a)

Summary of the working condition for Type B fan with a shroud running in the low speed regime

Measurement location		Working conditions		
x (m)	y (m)	Flow rate (CFM)	Δp (inch-water)	Speed (r.p.m.)
2·0	0·5	635	0·438	1411

TABLE 7(b)

Summary of the calculated and measured first two discrete sounds and the overall SPL values for Type B fan with a shroud running in the low speed regime

Peak number	Frequency (Hz)	Measured SPL (dBL)	Calculated SPL (dBL)	Difference SPL (dBL)
1	211·7	59·9	59·3	−0·6
2	423·3	48·9	50·3	+1·4
Total SPL (dBA)	0 ~ 6400	60·5	59·6	−0·9

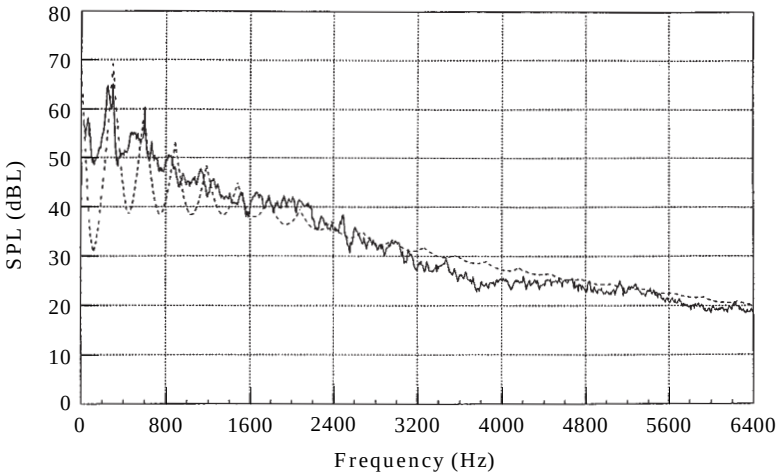

Figure 11. Comparison of the calculated and measured noise spectra from Type B fan with a shroud and radiator/condenser assembly running in the high speed regime: —, measured; - - - , calculated.

spectra of Type E fan are calculated under exactly the same conditions as those specified by the Bosch engineers. Tables 14(a–b) and 15(a–b) show the working conditions and differences between the calculated and measured SPL values for the BPF and overall sounds in A-weighting. Satisfactory results are obtained for all the fan assemblies tested.

6. EXAMINATION OF DESIGN PARAMETERS

Equation (12) can be used to assess the performance of an engine cooling fan assembly, given its characteristic dimensions and working conditions. As a further check of its validity, equation (12) is used to calculate the overall SPL values of dimensionally similar fans which are compared with those predicted by the fan laws currently in use by the design

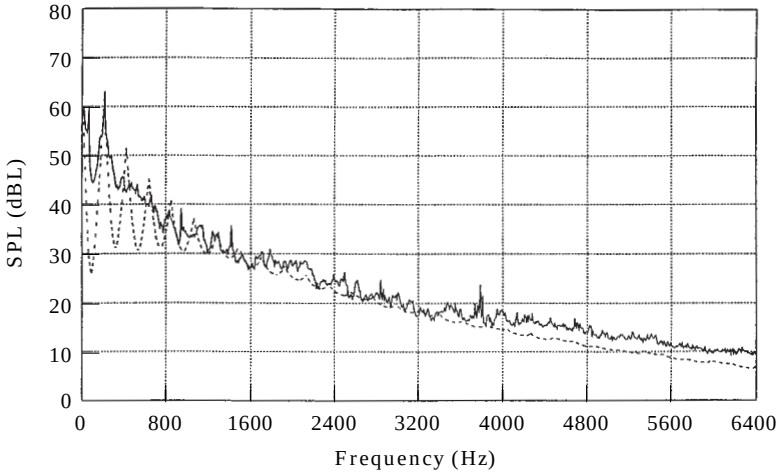

Figure 12. Comparison of the calculated and measured noise spectra from Type B fan with a shroud and radiator/condenser assembly running in the low speed regime: —, measured; - - - , calculated.

TABLE 8(a)

Summary of the working condition for Type B fan with a shroud and radiator/condenser assembly running in the high speed regime

Measurement location		Working conditions		
x (m)	y (m)	Flow rate (CFM)	Δp (inch-water)	Speed (r.p. m.)
2·0	0·5	1750	0·439	1997

TABLE 8(b)

Summary of the calculated and measured first two discrete sounds and the overall SPL values for Type B fan with a shroud and radiator/condenser assembly running in the high speed regime

Peak number	Frequency (Hz)	Measured SPL (dBL)	Calculated SPL (dBL)	Difference SPL (dBL)
1	299·6	65·3	68·3	+3·0
2	599·1	60·3	59·3	−1·0
Total SPL (dBA)	0 ~ 6400	71·4	71·8	+0·4

engineers. These fan laws are developed from the similitude principles and are applicable to dimensionally similar fans under different working conditions.

The fan laws can be written in two forms, one governing the flow rate, diameter, and speed and the other governing the static pressure drop, diameter, and speed of dimensionally similar fans:

$$Q_1 = Q_2\left(\frac{D_1}{D_2}\right)^3\left(\frac{N_1}{N_2}\right), \qquad Press_1 = Press_2\left(\frac{D_1}{D_2}\right)^2\left(\frac{N_1}{N_2}\right)^2, \tag{16, 17}$$

TABLE 9(a)

Summary of the working condition for Type B fan with a shroud and radiator/condenser assembly running in the low speed regime

Measurement location		Working conditions		
x (m)	y (m)	Flow rate (CFM)	Δp (inch-water)	Speed (r.p. m.)
2·0	0·5	1155	0·282	1425

TABLE 9(b)

Summary of the calculated and measured first two discrete sounds and the overall SPL values for Type B fan with a shroud and radiator/condenser running in the low speed regime

Peak number	Frequency (Hz)	Measured SPL (dBL)	Calculated SPL (dBL)	Difference SPL (dBL)
1	213·8	63·0	60·0	−3·0
2	427·5	45·0	51·0	+7·0
Total SPL (dBA)	0 ~ 6400	61·3	60·4	−0·9

TABLE 10(a)

Summary of the working condition for Type C fan with a shroud running in the high speed regime

Measurement location		Working conditions		
x (m)	y (m)	Flow rate (CFM)	Δp (inch-water)	Speed (r.p.m.)
1·0	0·0	901	0·840	2202

TABLE 10(b)

Summary of the calculated and measured SPL values of the BPF and overall sounds in A-weighting for Type C fan with a shroud running in the high speed regime

	Frequency (Hz)	Measured SPL (dBA)	Calculated SPL (dBA)	Difference SPL (dBA)
BPF	336·0	65·5	64·6	−0·9
Total	0 ∼ 6400	75·6	74·4	−1·2

where $Q_{1,2}$, $D_{1,2}$, $N_{1,2}$ and $Press_{1,2}$ represent the flow rates, blade diameters, speeds, and static pressure drops, respectively, and the subscripts 1 and 2 indicate the fan under design and that under test, respectively.

For example, let us consider a fan whose geometries and dimensions are specified. In particular, the diameter, flow rate, speed, and the static pressure drop of this fan are D_2, Q_2, N_2, and $Press_2$, respectively. Suppose that one decides to change the flow rate to Q_1 and the diameter to D_1, while keeping other geometries and dimensions constant. In order

TABLE 11(a)

Summary of the working condition for Type C fan with a shroud running in the low speed regime

Measurement location		Working conditions		
x (m)	y (m)	Flow rate (CFM)	Δp (inch-water)	Speed (r.p.m.)
1·0	0·0	609	0·46	1887

TABLE 11(b)

Summary of the calculated and measured SPL values of the BPF and overall sounds in A-weighting for Type C fan with a shroud running in the low speed regime

	Frequency (Hz)	Measured SPL (dBA)	Calculated SPL (dBA)	Difference SPL (dBA)
BPF	288·0	62·0	60·4	−1·6
Total	0 ∼ 6400	72·1	70·1	−2·0

TABLE 12(a)

Summary of the working condition for Type D fan with a shroud running in the high speed regime

Measurement location		Working conditions		
x (m)	y (m)	Flow rate (CFM)	Δp (inch-water)	Speed (r.p.m.)
1·0	0·0	1480	0·47	1902

TABLE 12(b)

Summary of the calculated and measured SPL values of the BPF and overall sounds in A-weighting for Type D fan with a shroud running in the high speed regime

	Frequency (Hz)	Measured SPL (dBA)	Calculated SPL (dBA)	Difference SPL (dBA)
BPF	288·0	61·6	64·0	+2·4
Total	0 ~ 6400	76·2	74·6	−1·6

to deliver the flow rate Q_1 with diamter D_1, one must run this fan at a different speed N_1, which can be determined by equation (16):

$$N_1 = N_2\left(\frac{Q_1}{Q_2}\right)\left(\frac{D_2}{D_1}\right)^3 .$$

The static pressure drop $Press_1$ will also change accordingly, which can be calculated by using equation (17). Note that equations (16) and (17) are valid for fans with identical geometry and shape. The only admissible variables are the diameter, flow rate, speed, and static pressure drop.

TABLE 13(a)

Summary of the working condition for Type D fan with a shroud running in the low speed regime

Measurement location		Working conditions		
x (m)	y (m)	Flow rate (CFM)	Δp (inch-water)	Speed (r.p.m.)
1·0	0·0	1345	0·20	1771

TABLE 13(b)

Summary of the calculated and measured SPL values of the BPF and overall sounds in A-weighting for Type D fan with a shroud running in the low speed regime

	Frequency (Hz)	Measured SPL (dBA)	Calculated SPL (dBA)	Difference SPL (dBA)
BPF	272·0	61·7	62·4	+0·7
Total	0 ~ 6400	74·4	73·0	−1·4

TABLE 14(a)

Summary of the working condition for Type E fan with a shroud running in the high speed regime

Measurement location		Working conditions		
x (m)	y (m)	Flow rate (CFM)	Δp (inch-water)	Speed (r.p.m.)
1·0	0·0	2536	0·33	1600

TABLE 14(b)

Summary of the calculated and measured SPL values of the BPF and overall sounds in A-weighting for Type E fan with a shroud running in the high speed regime

	Frequency (Hz)	Measured SPL (dBA)	Calculated SPL (dBA)	Difference SPL (dBA)
BPF	160·0	64·7	57·2	−7·5
Total	0 ∼ 6400	68·0	67·9	−0·1

Using equations (16) and (17), the changes in the total SPL values of a cooling fan assembly due to changes in fan speeds or diameters can then be estimated:

$$\Delta\text{SPL} = 20 \log \left(\frac{D_1}{D_2}\right)^{3\cdot5} + 20 \log \left(\frac{N_1}{N_2}\right)^{2\cdot5}, \tag{18a}$$

or due to changes in fan diameters or static pressure drops:

$$\Delta\text{SPL} = 20 \log \left(\frac{D_1}{D_2}\right) + 20 \log \left(\frac{Press_1}{Press_2}\right)^{1\cdot25}. \tag{18b}$$

TABLE 15(a)

Summary of the working condition for Type E fan with a shroud running in the low speed regime

Measurement location		Working conditions		
x (m)	y (m)	Flow rate (CFM)	Δp (inch-water)	Speed (r.p.m.)
1·0	0·0	1419	0·27	1413

TABLE 15(b)

Summary of the calculated and measured SPL values of the BPF and overall sounds in A-weighting for Type E fan with a shroud running in the low speed regime

	Frequency (Hz)	Measured SPL (dBA)	Calculated SPL (dBA)	Difference SPL (dBA)
BPF	122·6	56·3	53·1	−3·2
Total	0 ∼ 6400	65·8	63·8	−2·0

TABLE 16

Examination of design parameters for Type C fan assembly

	D (mm)	*Q* (CFM)	*N* (r.p.m.)	*Press* (IWC)	BPF (dBL)	Total (dBA)	Total (dBL)
Under test	388	1300	2185	0·69	71·2	74·6	81·4
Under design	388	1400	2353	0·80	72·8	76·9	83·0
Changes	0·0	+100	+170	+0·11	+1·6	+2·3	+1·6

In what follows, Types C, D and E fans are considered and the effects of the blade diameter, speed, flow rate, and static pressure on the changes in the total SPL values are examined.

Table 16 displays the case of Type C fan which has a diamter $D_2 = 388$ mm and a required CFM value $Q_2 = 1300$ under a speed $N_2 = 2185$ r.p.m. and a static pressure drop $Press_2 = 0{\cdot}69$ inch-water. Using equation (12), we can calculate the noise spectrum and find 71·2 dB for the BPF and 81·4 dB for the total SPL value. Now, the CFM requirement is changed to $Q_1 = 1400$ (an increase of 7·7%), while fixing the diameter at $D_1 = 388$ mm. In order to deliver this higher CFM value, the fan must run faster. The new speed can be calculated by using equation (16), $N_1 = N_2(Q_1/Q_2) = 2353$ r.p.m. This new speed will bring about a new static pressure drop which can be determined by equation (17), $Press_1 = Press_2(N_1/N_2)^2 = 0{\cdot}80$ inch-water. Once N_1 and $Press_1$ are known, the noise spectrum can be calculated again. The new SPL value for the BPF is found to be 72·8 dB and that for the total sound to be 83·0 dB. Figure 13 depicts the changes in the noise spectrum due to changes in the flow rate and static pressure drop. In this case, the change in the SPL value for the BPF and that for the total sound are both equal to +1·6 dB.

The change in the total SPL value due to the change in the flow rate and static pressure drop can also be obtained by using equation (18). Here $D_1 = D_2 = 388$ mm, $Q_2 = 1300$, $Q_1 = 1400$, $N_2 = 2185$ r.p.m., and $Press_2 = 0{\cdot}69$ inch-water. Using equation (16), one finds

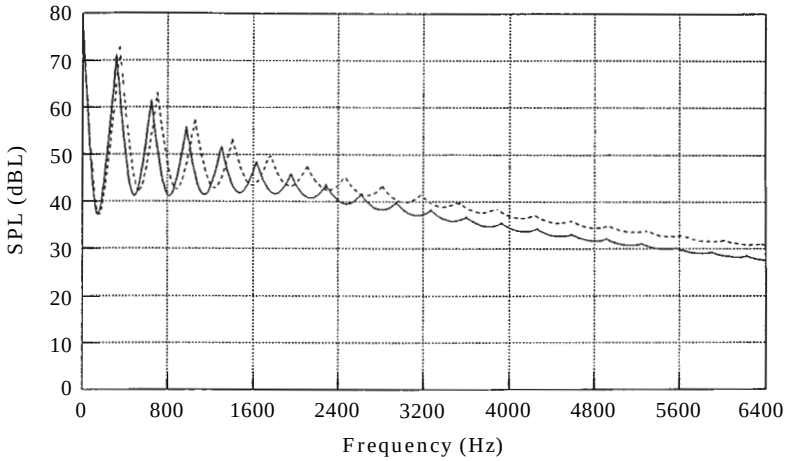

Figure 13. Comparison of the noise spectra of Type C fans due to changes in flow rate and static pressure drop: —, under test; - - - , under design.

TABLE 17

Effects of changing design parameters of Type C fan on resulting noise levels

	D (mm)	Q (CFM)	N (r.p.m.)	*Press* (IWC)	BPF (dBL)	Total (dBA)	Total (dBL)	ΔSPL (dBL)	Fan laws (dBL)
Test	388	1300	2186	0·69	71·2	74·6	81·4	+0·0	+0·0
Design	388	1400	2353	0·80	72·8	76·9	83·0	+1·6	+1·6
Design	388	1500	2521	0·92	74·2	79·0	84·5	+3·1	+3·1
Design	388	1600	2689	1·1	75·5	80·8	85·9	+4·5	+4·5
Test	420	1300	1723	0·50	72·7	73·9	82·0	+0·0	+0·0
Design	420	1400	1855	0·58	74·4	76·3	83·9	+1·8	+1·6
Design	420	1500	1988	0·67	77·8	80·4	87·7	+5·7	+3·1
Design	420	1600	2120	0·76	77·3	80·5	87·0	+4·9	+4·5
Test	450	1300	1401	0·38	72·7	71·9	81·2	+0·0	+0·0
Design	450	1400	1508	0·44	74·4	74·3	83·0	+1·8	+1·6
Design	450	1500	1616	0·51	76·0	76·6	84·7	+3·5	+3·1
Design	450	1600	1724	0·58	77·4	78·7	86·3	+5·1	+4·5
Test	500	1300	1021	0·25	68·8	64·7	75·9	+0·0	+0·0
Design	500	1400	1100	0·29	70·5	67·2	77·9	+2·1	+1·6
Design	500	1500	1178	0·33	72·1	69·6	79·6	+3·7	+3·1
Design	500	1600	1257	0·38	73·6	71·8	81·3	+5·4	+4·5

$N_1 = 2353$ r.p.m. and $Press_1 = 0{\cdot}80$ inch-water. Substituting D_1, D_2, N_1 and N_2 into equation (18a) then yields

$$\Delta\text{SPL} = 20 \log \left(\frac{388}{388}\right)^{3{\cdot}5} + 20 \log \left(\frac{2353}{2185}\right)^{2{\cdot}5} = +1{\cdot}6 \text{ dB(L)}.$$

Similarly, substituting D_1, D_2, $Press_1$ and $Press_2$ into equation (18b), one obtains

$$\Delta\text{SPL} = 20 \log \left(\frac{388}{388}\right) + 20 \log \left(\frac{0{\cdot}80}{0{\cdot}69}\right)^{1{\cdot}25} = +1{\cdot}6 \text{ dB(L)},$$

which agrees perfectly with our calculation.

Table 17 summarizes the results of examinations of the effects of changing blade diameters D_i, flow rates Q_i, speeds N_i, and static pressure drops $Press_i$ on the changes in the total SPL values. Note that the last two columns in Table 17 represent the calculated ΔSPL values by using equation (12) and those predicted by the fan laws, respectively. Good agreements are obtained in all cases.

Next, we consider Type D fan. In particular, for the fan under test we have $D_2 = 418$ mm, $Q_2 = 1550$, $N_2 = 1990$, and $Press_2 = 0{\cdot}48$ inch-water. The resulting noise spectrum can be calculated by equation (12). Suppose now that the diameter is increased to $D_1 = 450$ mm (a 7·8% increase), while keeping the flow rate constant. Since the new fan can deliver more flow with a larger diameter and since the flow rate requirement remains the same, the fan speed can be reduced. Using equation (16), one finds $N_1 = N_2(D_2/D_1)^3 = 1595$ r.p.m. (a 19·8% reduction). The static pressure drop changes accordingly, $Press_1 = Press_2(D_1/D_2)^2(N_1/N_2)^2 = 0{\cdot}357$ inch-water. Because of a drop in fan speed, the overall noise level is reduced. Figure 14 illustrates the comparison of the noise spectra of the fan under test and that under design. Table 18 lists the changes in the design parameters and those in the SPL values for the BPF and the total sound. Results show

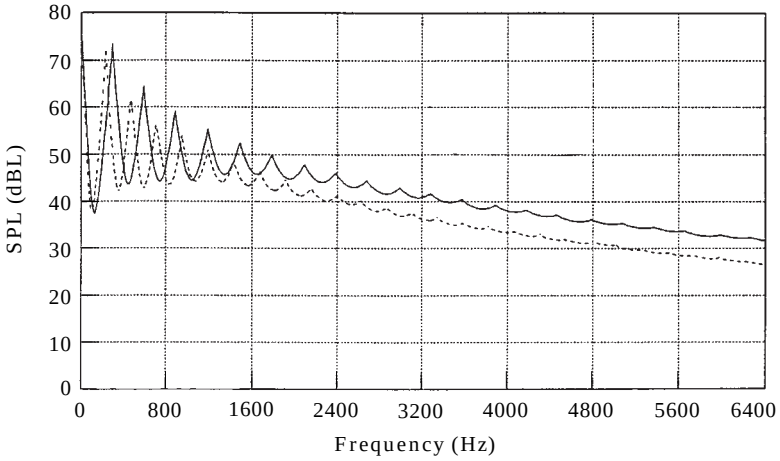

Figure 14. Comparison of the noise spectra of Type D fans due to changes in diameter and static pressure drop: —, under test; - - - , under design.

that increasing the fan diameter to $D_1 = 450$ mm reduces the SPL for the BPF by 1·5 dB and that for the total sound by 2·3 dB.

The change in the total SPL value can also be obtained by using equation (18). Here $D_2 = 418$ mm, $D_1 = 450$ mm, $Q_2 = Q_1 = 1550$, $N_2 = 1990$ r.p.m., $N_1 = 1595$ r.p.m., $Press_2 = 0{\cdot}480$ inch-water, and $Press_1 = 0{\cdot}357$ inch-water. Substituting these quantities into equation (18) leads to

$$\Delta\text{SPL} = 20 \log \left(\frac{450}{418}\right)^{3{\cdot}5} + 20 \log \left(\frac{1595}{1990}\right)^{2{\cdot}5} = -2{\cdot}6 \text{ dB(L)},$$

$$\Delta\text{SPL} = 20 \log \left(\frac{450}{418}\right) + 20 \log \left(\frac{0{\cdot}357}{0{\cdot}480}\right)^{1{\cdot}25} = -2{\cdot}6 \text{ dB(L)},$$

which are in good agreement with those predicted by our computer model. Table 19 demonstrates the comparison of the changes in the total SPL values predicted by our computer model for Type D fan under various design parameters and those predicted by the fan laws. Results show that favorable agreements are obtained in all cases.

Finally, the prototype fan model Type E is considered. The fan under test has a diameter $D_2 = 450$ mm and a required flow rate $Q_2 = 1900$ at $N_2 = 1880$ r.p.m. and $Press_2 = 0{\cdot}500$ inch-water. Using the company supplied data, the resulting noise spectrum can be calculated (see Figure 15). Suppose now that the fan diameter is increased to

TABLE 18

Examination of design parameters for Type D fan assembly

	D (mm)	*Q* (CFM)	*N* (r.p.m.)	*Press* (IWC)	BPF (dBL)	Total (dBA)	Total (dBL)
Under test	418	1550	1990	0·480	73·4	76·9	82·4
Under design	450	1550	1595	0·357	71·9	73·3	80·1
Changes	+32	0·0	−395	−0·123	−1·5	−3·6	−2·3

TABLE 19

Effects of changing design parameters of Type D fan on resulting noise levels

	D (mm)	*Q* (CFM)	*N* (r.p.m.)	*Press* (IWC)	BPF (dBL)	Total (dBA)	Total (dBL)	ΔSPL (dBL)	Fan laws (dBL)
Test	418	1550	1990	0·48	73·4	76·9	82·4	+0·0	+0·0
Design	418	1650	2118	0·54	74·8	78·8	84·0	+1·6	+1·4
Design	418	1750	2247	0·61	76·2	80·7	85·4	+3·0	+2·6
Design	418	1850	2375	0·68	77·4	82·4	86·8	+4·4	+3·8
Test	450	1550	1595	0·36	71·9	73·2	80·1	+0·0	+0·0
Design	450	1650	1698	0·41	73·4	75·4	81·7	+1·6	+1·3
Design	450	1750	1801	0·46	74·7	77·3	83·2	+3·1	+2·6
Design	450	1850	1904	0·51	76·0	79·1	84·6	+4·5	+3·8
Test	480	1550	1314	0·28	69·6	69·3	77·1	+0·0	+0·0
Design	480	1650	1399	0·31	71·1	71·4	78·6	+1·6	+1·4
Design	480	1750	1484	0·35	72·5	73·3	80·3	+3·2	+2·6
Design	480	1850	1569	0·39	73·8	75·2	81·7	+4·6	+3·9
Test	510	1550	1096	0·22	67·4	65·4	74·1	+0·0	+0·0
Design	510	1650	1166	0·25	68·9	67·4	75·8	+1·7	+1·3
Design	510	1750	1237	0·28	70·3	69·5	77·2	+3·2	+2·6
Design	510	1850	1308	0·31	71·7	71·4	78·8	+4·7	+3·8

$D_1 = 490$ mm and the required flow rate is increased to $Q_1 = 2000$ in order to ascertain how they impact on the fan noise performance. To this end, first the fan speed and static pressure drop under the new design are calculated. Using equations (16) and (17), one finds $N_1 = N_2(Q_1/Q_2)(D_2/D_1)^3 = 1533$ r.p.m. and $Press_1 = Press_2(D_1/D_2)^2(N_1/N_2)^2 = 0{\cdot}394$ inch-water. Substituting these quantities into equation (12) yields a new noise spectrum (see Figure 15). The results show that increasing the diameter by 8·9% and the flow rate by 5·3% causes the fan speed to drop by 18·5%. These changes lead to reduction in the SPL values for both the BPF and total sound. Table 20 indicates that the SPL value for the BPF is reduced by 3·3 dB, whereas that for the total sound is reduced by 3·0 dB.

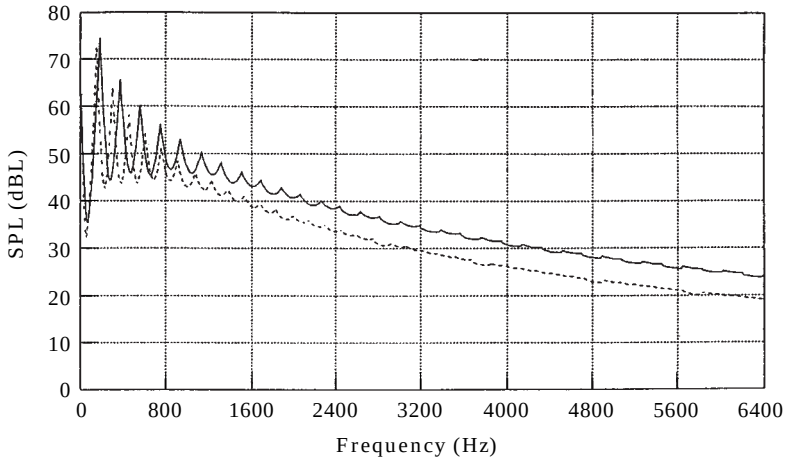

Figure 15. Comparison of the noise spectra of Type E fans due to changes in diameter, flow rate and static pressure drop: —, under test; - - - , under design.

TABLE 20

Examination of design parameters for Type E fan assembly

	D (mm)	*Q* (CFM)	*N* (r.p.m.)	*Press* (IWC)	BPF (dBL)	Total (dBA)	Total (dBL)
Under test	450	1900	1880	0·500	74·5	73·4	80·1
Under design	490	2000	1533	0·394	72·3	69·4	77·1
Changes	+40	+100	−347	−0·106	−3·3	−4·0	−3·0

The change in the SPL value for the total sound can also be calculated by using the fan laws. Substituting the values of $D_{1,2}$ and $N_{1,2}$ into equation (18a), one obtains ΔSPL due to changes in the fan speed and diameter as

$$\Delta\text{SPL} = 20 \log \left(\frac{490}{450}\right)^{3\cdot5} + 20 \log \left(\frac{1533}{1880}\right)^{2\cdot5} = -1\cdot8 \text{ dB(L)}.$$

Similarly, substituting $D_{1,2}$ and $Press_{1,2}$ into equation (18b) yields ΔSPL due to changes in the fan diameter and static pressure drop as

$$\Delta\text{SPL} = 20 \log \left(\frac{490}{450}\right) + 20 \log \left(\frac{0\cdot394}{0\cdot500}\right)^{1\cdot25} = -1\cdot8 \text{ dB(L)},$$

which is close to that given by equation (12). Table 21 summarizes the comparisons of the changes in the total SPL values for Type E fan under various design parameters with those predicted by the fan laws. Good agreements are obtained in all cases.

TABLE 21

Effects of changing design parameters of Type E fan on resulting noise levels

	D (mm)	*Q* (CFM)	*N* (r.p.m.)	*Press* (IWC)	BPF (dBL)	Total (dBA)	Total (dBL)	ΔSPL (dBL)	Fan laws (dBL)
Test	450	1900	1880	0·50	74·5	73·4	80·1	+0·0	+0·0
Design	450	2000	1979	0·55	75·6	75·0	81·5	+1·4	+1·1
Design	450	2100	2078	0·61	76·7	76·5	82·8	+2·7	+2·2
Design	450	2200	2177	0·67	77·7	78·1	83·9	+3·8	+3·2
Test	490	1900	1456	0·36	71·1	67·7	75·7	+0·0	+0·0
Design	490	2000	1533	0·39	72·3	69·4	77·1	+1·4	+1·1
Design	490	2100	1609	0·43	73·4	71·0	78·4	+2·7	+2·2
Design	490	2200	1686	0·48	74·5	72·6	79·7	+4·0	+3·2
Test	530	1900	1151	0·26	67·8	62·1	71·7	+0·0	+0·0
Design	530	2000	1211	0·29	69·0	63·9	73·1	+1·4	+1·1
Design	530	2100	1272	0·32	70·2	65·4	74·5	+2·8	+2·2
Design	530	2200	1332	0·35	71·3	67·1	75·7	+4·1	+3·2
Test	570	1900	925	0·19	64·7	56·8	67·9	+0·0	+0·0
Design	570	2000	974	0·22	65·9	58·7	69·3	+1·3	+1·1
Design	570	2100	1022	0·24	67·1	60·2	70·7	+2·8	+2·2
Design	570	2200	1071	0·26	68·2	62·0	71·9	+4·0	+3·2

It is worth pointing out, however, that the fan laws are capable of predicting the changes in the overall SPL values only for dimensionally similar fans due to changes in the diameters, flow rates, speeds, and static pressure drops, while equation (12) can predict not only the overall SPL values, but also noise spectra for changes in the fan blade geometries, dimensions, and working conditions.

7. CONCLUSIONS

A computer model for estimating the noise performance of an engine cooling fan assembly is developed. In this model, the effect of a fan shroud on the discrete sounds centered at the BPF and its harmonics, that of an upstream radiator/condenser set on the broadband sounds, and that of an engine compartment on the overall noise spectrum are taken into account. The computer model thus obtained is validated experimentally on five sets of completely different engine cooling fan assemblies. In all cases the calculated noise spectra compare well with measured data taken in the AVNC Laboratory at Wayne State and taken independently by the engineers at the Robert Bosch Company in Boston. The major conclusions are as follows.

This computer program enables one to assess the noise performance of engine cooling fans that are similar in sizes and shapes to those tested.

Unlike the fan laws that can predict the changes in the overall SPL values due to changes in sizes and speeds or changes in sizes and static pressure drops, the present computer program can predict changes in the noise spectra, including the overall SPL values due to changes in blade geometries, dimensions, and working conditions.

While the present computer program can capture the main characteristics of cooling fan noise spectra, it is still not generalized for any type of fan assemblies because many coefficients such as a_i, $i = 1$–4, are fixed as constants.

In order to extend this computer model to any cooling fan assembly, these coefficients must be correlated to the design parameters of the shroud, radiator/condenser, and engine compartment.

ACKNOWLEDGMENT

The work was supported by Ford Motor Company.

REFERENCES

1. S. F. Wu, S. Su and H. Shah 1997 *Journal of Sound and Vibration* **200**, 379–399. Modeling of noise spectrum from an axial flow fan in free space.
2. I. J. Sharland 1964 *Journal of Sound and Vibration* **1**, 302–322. Sources of noise in axial flow fans.
3. C. G. Van Niekerk 1966 *Journal of Sound and Vibration* **3**, 46–56. Noise generation in axial flow fans.
4. N. Le and S. Filleul 1966 *Journal of Sound and Vibration* **3**, 147–165. An investigation of axial flow fan noise.
5. P. E. Doak and P. G. Vaidya 1969 *Journal of Sound and Vibration* **9**, 192–196. A note on the relative importance of discrete frequency and broad-band noise generating mechanisms in axial fans.
6. J. E. Ffowcs Williams and D. L. Hawkings 1969 *Journal of Sound and Vibration* **10**, 10–21. Theory relating to the noise of rotating machinery.
7. M. V. Lowson and J. B. Ollerhead 1969 *Journal of Sound and Vibration* **9**, 197–222. A theoretical study of helicopter rotor noise.

8. S. E. Wright 1969 *Journal of Sound and Vibration* **9**, 223–240. Sound radiation from a lifting rotor generated by asymmetric disk loading.
9. S. E. Wright 1971 *Journal of Sound and Vibration* **17**, 437–498. Discrete radiation from rotating periodic sources.
10. B. D. Mugridge 1969 *Journal of Sound and Vibration* **10**, 227–246. The measurement of spinning acoustic modes generated in an axial flow fan.
11. B. D. Mugridge 1976 *Journal of Sound and Vibration* **44**, 349–367. The noise of cooling fans used in heavy automotive vehicles.
12. N. Chandrashekhara 1970 *Journal of Sound and Vibration* **13**, 43–49. Experimental studies of discrete tone noise from an axial flow fan.
13. N. Chandrashekhara 1971 *Journal of Sound and Vibration* **18**, 533–543. Tone radiation from axial flow fans running in turbulent flow.
14. N. Chandrashekhara 1971 *Journal of Sound and Vibration* **19**, 133–146. Sound radiation from inflow turbulence in axial flow fans.
15. B. Barry and C. J. Moore 1971 *Journal of Sound and Vibration* **17**, 207–220. Subsonic fan noise.
16. H. H. Hubbard, D. L. Lansing and H. L. Runyan 1971 *Journal of Sound and Vibration* **19**, 227–249. A review of rotating blade noise technology.
17. C. L. Morfey and H. K. Tanna 1971 *Journal of Sound and Vibration* **15**, 325–351. Sound radiation from a point force in circular motion.
18. C. L. Morfey 1972 *Journal of Sound and Vibration* **22**, 445–466. The acoustics of axial flow machines.
19. C. L. Morfey 1972 *Journal of Sound and Vibration* **23**, 291–295. The sound field of sources in motion.
20. C. L. Morfey 1973 *Journal of Sound and Vibration* **28**, 587–617. Rotating blades and aerodynamic sound.
21. R. H. F. Pao 1967 *Fluid Mechanics*. Charles E. Merrill Books. See pp. 256–262.